THE JOURNAL OF BIOLOGICAL CHEMISTRY VOL. 285, NO. 12, pp. 9221–9232, March 19, 2010

Orphan Nuclear Receptor DAX-1 Acts as a Novel Corepressor of Liver X Receptor α and Inhibits Hepatic Lipogenesis*[S]

Received for publication, October 6, 2009, and in revised form, January 7, 2010 Published, JBC Papers in Press, January 15, 2010, DOI 10.1074/jbc.M109.073650

Balachandar Nedumaran[‡1], Gwang Sik Kim[‡1], Sungpyo Hong[§], Young-Sil Yoon[§], Yong-Hoon Kim[¶], Chul-Ho Lee[¶], Young Chul Lee[‡2], Seung-Hoi Koo[§3], and Hueng-Sik Choi[‡‖4]

From the [‡]Hormone Research Center, School of Biological Science and Technology, Chonnam National University, Gwangju 500-757, the [‖]Department of Biomedical Sciences, Research Institute of Medical Sciences, Chonnam National University Medical School, Gwangju 501-746, the [§]Department of Molecular Cell Biology, Sungkyunkwan University School of Medicine, Suwon 440-746, and the [¶]Korea Research Institute of Bioscience and Biotechnology, Daejeon 305-806, Korea

DAX-1 (dosage-sensitive sex reversal adrenal hypoplasia congenital critical region on X chromosome, gene 1) is a member of the nuclear receptor superfamily that can repress diverse nuclear receptors and has a key role in adreno-gonadal development. Our previous report has demonstrated that DAX-1 can inhibit hepatocyte nuclear factor 4α transactivity and negatively regulate gluconeogenic gene expression (Nedumaran, B., Hong, S., Xie, Y. B., Kim, Y. H., Seo, W. Y., Lee, M. W., Lee, C. H., Koo, S. H., and Choi, H. S. (2009) *J. Biol. Chem.* 284, 27511–27523). Here, we further expand the role of DAX-1 in hepatic energy metabolism. Transfection assays have demonstrated that DAX-1 can inhibit the transcriptional activity of nuclear receptor liver X receptor α (LXRα). Physical interaction between DAX-1 and LXRα was confirmed Immunofluorescent staining in mouse liver shows that LXRα and DAX-1 are colocalized in the nucleus. Domain mapping analysis shows that the entire region of DAX-1 is involved in the interaction with the ligand binding domain region of LXRα. Competition analyses demonstrate that DAX-1 competes with the coactivator SRC-1 for repressing LXRα transactivity. Chromatin immunoprecipitation assay showed that endogenous DAX-1 recruitment on the *SREBP-1c* gene promoter was decreased in the presence of LXRα agonist. Overexpression of DAX-1 inhibits T7-induced LXRα target gene expression, whereas knockdown of endogenous *DAX-1* significantly increases T7-induced LXRα target gene expression in HepG2 cells. Finally, overexpression of *DAX-1* in mouse liver decreases T7-induced LXRα target gene expression, liver triglyceride level, and lipid accumulation. Overall, this study suggests that DAX-1, a novel corepressor of LXRα, functions as a negative regulator of lipogenic enzyme gene expression in liver.

Nuclear receptors are a class of DNA binding transcription factors that regulate gene expression and play important roles in a variety of biological and pathological processes (2). Orphan nuclear receptor DAX-1 (NROB1) is an unusual member of the nuclear receptor superfamily (3). The C-terminal region has the structure that is characteristic of a ligand binding domain (LBD).[5] Unlike other nuclear receptors, the N-terminal region does not have any classical DNA binding domain. However, it has three short repeats (65–67 amino acids) each containing an L*XX*LL-related motif. Duplication of the *DAX-1* gene is associated with male to female reversal in XY individuals, and mutations in *DAX-1* are responsible for adrenal hypoplasia congenita, an inherited disorder of adrenal gland development (4). DAX-1 generally acts as a negative regulator to repress the transcriptional activity of receptors such as estrogen receptor, thyroid receptor β, steroidogenic factor (SF-1), androgen receptor, estrogen receptor-related receptor γ, glucocorticoid receptor, nerve growth factor-inducible gene B (Nur77), and peroxisome proliferator-activated receptor γ (PPARγ) (5–12). We have previously reported that DAX-1 can negatively regulate the expression of gluconeogenic genes by inhibiting the transcriptional activity of hepatocyte nuclear factor 4 α (HNF4α) (1). DAX-1 is also known to interact with and inhibit the transcriptional activity of transcription factors, including OCT3/4 (13). DAX-1 has been shown to compete with nuclear receptor coactivators such as PGC-1α (11), GRIP-1 (10), and SRC-1 (11), and it is also known to recruit corepressors such as NCoR and Alien (9). A recent report showing the three-dimensional structure of DAX-1 reveals that Dax-1 could function as a ligand-independent nuclear receptor as well as a competitive transcriptional corepressor (14).

Liver X receptor α (LXRα) is a member of the nuclear receptor superfamily that heterodimerizes with retinoid X receptor (RXR). LXRα/RXR heterodimers bind to DR-4-type response elements known as the LXR-response elements (LXRE) in their target genes. LXRα is abundantly expressed in tissues with

* This work was supported in part by the Korea Science and Engineering Foundation through the National Research Laboratory Program funded by the Ministry of Science and Technology Grant M10500000047-06J0000-04710.

[S] The on-line version of this article (available at http://www.jbc.org) contains supplemental Figs. 1–4.

[1] Both authors contributed equally to this work.

[2] Supported by Basic Science Research Program Grant 2009-0088438 from the National Research Foundation.

[3] Supported by Korea Science and Engineering Foundation Grant R01-2008-000-11935-0, Korea Research Foundation Grant 2006-E00037 from the Ministry of Education, Science and Technology, and a grant from Marine Biotechnology Program funded by Ministry of Land, Transport, and Maritime Affairs, Republic of Korea. To whom correspondence may be addressed: Hormone Research Center, Chonnam National University, Kwangju, 500-757 Korea. E-mail: hsc@chonnam.ac.kr.

[4] To whom correspondence may be addressed: Dept. of Molecular Cell Biology, Sungkyunkwan University School of Medicine, 300 Chunchun-dong, Jangan-gu, Suwon, 440-746, South Korea. E-mail: shkoo@med.skku.ac.kr.

[5] The abbreviations used are: LBD, ligand binding domain; SHP, small heterodimer partner; HNF4α, hepatocyte nuclear factor 4α; FAS, fatty-acid synthase; NCoR, nuclear receptor corepressor; ChREBP, carbohydrate-response element-binding protein; PBS, phosphate-buffered saline; MBP, maltose-binding protein; HA, hemagglutinin; GST, glutathione *S*-transferase; GFP, green fluorescent protein; LXRα, liver X receptor α; WT, wild type; PPAR, peroxisome proliferator-activated receptor; RT, reverse transcription; RXR, retinoid X receptor; LXRE, LXR-response element.

active lipid metabolism, such as white adipose tissue, liver, intestine, and macrophages, whereas the LXRβ isoform is more ubiquitously expressed (15). Both *LXRα* and *LXRβ* are stimulated by several natural and synthetic ligands, including (20*S*)-hydroxycholesterol, (22*R*)-hydroxycholesterol, 24-hydroxycholesterol, T0314407, T0901317, and GW3965 (16). It has been reported that the p160 coactivator SRC-1 and p300 can bind to the *ABCA1* promoter via the oxysterol-induced LXRα/RXR heterodimer and cause maximal activation of promoter (17). A recent study has demonstrated that SIRT1 deacetylates and activates the nuclear receptor LXRα by favoring its ligand-dependent proteasomal degradation, thereby potentially regulating reverse cholesterol transport (18). In the unliganded state, LXRα preferentially associates with corepressors such as the nuclear receptor corepressor (NCoR) and silent mediator of retinoic acid receptor and thyroid receptor (SMRT) (19). Furthermore, decreased expression of NCoR has been shown to increase the expression of adipocyte-specific genes (20), and the recruitment of NCoR has also been shown to modulate LXR signaling in liver (21).

In liver, LXR is involved in transcriptional control of *Cyp7A1*, encoding a critical enzyme in the conversion of cholesterol into bile acids, as well as *ABCG5/ABCG*, encoding ABC transporters implicated in biliary cholesterol excretion. Induction of intestinal *ABCA1*, *ABCG5*, and *ABCG8* expression upon LXR activation accelerates fecal cholesterol disposal by reducing the efficiency of cholesterol absorption. LXR has also been reported to control genes that encode proteins involved in *de novo* lipogenesis. In particular, LXR is known to induce the expression of *SREBP-1c*, a transcription factor that regulates the expression of various lipogenic genes, including those encoding acetyl-coenzyme A carboxylase and fatty-acid synthase (FAS) (22). LXR is also known to regulate the expression of carbohydrate-response element-binding protein (ChREBP) (23). In addition, LXR is known to directly influence the transcription of genes encoding fatty acid synthase, lipoprotein lipase, cholesterol ester transfer protein, and stearoyl-CoA desaturase 1. Moreover, activation of LXRs by agonistic compounds induces the expression of enzymes involved in the synthesis of fatty acids in liver cells (24).

In this study, we show that DAX-1 inhibits the transcriptional activity of LXRα through direct interaction and competition with coactivator SRC-1. Overexpression of DAX-1 decreases the expression of *Srebp-1c,* FAS, and acetyl-coenzyme A carboxylase, whereas knockdown of endogenous DAX-1 increases the LXRα target gene expression. Finally, hepatic overexpression of DAX-1 decreases LXRα agonist-induced liver triglyceride level and lipid accumulation in mouse. Collectively, this study demonstrates that DAX-1 represses the transcriptional activity of LXRα to control the lipogenesis.

EXPERIMENTAL PROCEDURES

Materials and Plasmids—The synthetic LXR agonist TO901317 (T7) was purchased from Cayman Chemicals (Ann Arbor, MI). The reporter plasmids, LXRE-Luc and *SREBP-1c*-Luc, were described previously (25). LXRα WT, AB, C, DE, and DEΔAF2 were subcloned into pcDNA3-HA (Invitrogen) at BamHI and XhoI sites. GFP-hDAX-1 and FLAG-hDAX-1 were described previously (1). SRC-1 was subcloned in he pcDNA3-HA vector using EcoRI and XhoI sites. DAX-1 was subcloned into the pEBG (GST) vector using BamHI and NotI (1). MBP-LXRα WT, AB, C, DE, and DEΔAF2 were subcloned into pET28-MBP-HTa using BamHI and XhoI sites, whereas MBP-SHP and -DAX-1 were cloned into pET28-MBP-HTa using EcoRI and XhoI sites.

Preparation of Recombinant Adenovirus—For the ectopic expression of the transgene, the adenoviral vector systems were used as described previously (26). Briefly, the cDNA encoding FLAG-DAX-1 was cloned into the pAdTrack shuttle vector. The FLAG-DAX-1 fragment was digested with KpnI/XhoI and was cloned into the KpnI/XhoI site of the pAdTrack-CMV vector. Recombination of AdTrack-CMV-FLAG-DAX-1 with adenoviral gene carrier vector was performed by transformation into pretransformed AdEasy-BJ21-competent cells. Recombinant adenoviruses expressing GFP only or unspecific RNA interference control were described earlier. Oligonucleotides for DAX-1 small hairpin RNA (ctgtaccgctgctgcttctgcggagaa) were synthesized by IDT (Coralville, IA). Adenovirus for small hairpin DAX-1 was generated as described previously (1).

Cell Culture and Transient Transfection Assay—HepG2, 293T, and HeLa cells were maintained in Dulbecco's modified Eagle's medium, and AML12 cells were maintained in Dulbecco's modified Eagle's medium/F-12 (Invitrogen), supplemented with 10% fetal bovine serum (Cambrex Bio Science Walkersville, Inc., Walkersville, MD) and antibiotics (Invitrogen). Cells were split in 24-well plates at densities of $2–8 \times 10^4$ cells/well the day before transfection. Transient transfections were performed using the SuperFect transfection reagent (Qiagen, Valencia, CA) according to the manufacturer's instruction. Cells were cotransfected with indicated reporter plasmids together with expression vectors encoding various transcription factors. Total DNA used in each transfection was adjusted to 1 μg/well by adding appropriate amount of empty vector, and CMV-β-galactosidase plasmids were cotransfected as an internal control. Cells were harvested ~40–48 h after the transfection for luciferase and β-galactosidase assays. The luciferase activity was normalized with β-galactosidase activity. Knockdown of hDAX-1 by small interfering RNA and luciferase assays was performed as described previously (1).

Isolation and Culture of Primary Hepatocyte and Animal Experiments—Primary rat hepatocytes were prepared from 200- to 300-g Sprague-Dawley rats by the collagenase perfusion method as described previously (26). After attachment, cells were infected with adenoviruses for 16 h. Subsequently, cells were maintained in the serum-free Medium 199 media (Mediatech) overnight and treated with 100 nM dexamethasone and 10 μM forskolin for 2 h with or without 100 nM insulin for 16 h. Male 8-week-old C57BL/6 mice were provided with a standard rodent diet. T0901317 (LXR agonist, 50 mg/kg body weight) or vehicle (1% methylcellulose and 1% Tween 80) were administered by oral gavage each day for 1 week. Adenoviruses GFP or DAX-1 were delivered by tail vein injection on the 4th day of oral gavage. Three days after adenovirus injection, mice were sacrificed. Protein and RNA were extracted from the livers of each group for Western blot and real time quantitative RT-PCR

analyses, respectively. All experiments were conducted by the guideline of Sungkyunkwan University School of Medicine Institutional Animal Care and Use Committee (IACUC).

Quantitative RT-PCR—Total RNAs were extracted from either tissue samples or rat primary hepatocytes under various conditions using TRIzol reagent (Invitrogen) according to the manufacturer's protocol. DAX-1, PGC-1α, SREBP-1c, FAS and acetyl-coenzyme A carboxylase gene expressions were analyzed by quantitative RT-PCR as described previously (1, 26). The primers used for PCR of human/rat SREBP-1c, DAX-1, PGC-1α, FAS, ACC1α, and β-actin are as follows: human/mouse DAX-1, forward 5′-AGGGCAGCATCCTCTACAAC-3′ and reverse 5′-TGGTCTTCACCACAAAAGCA-3′; SRC-1, forward 5′-GTGGGTCCTGGACACTGACT-3′ and reverse 5′-AAAGTGAGCCGCAAGGTAGA-3′; PGC-1α, forward 5′-CTGGTTCCGGAAAGACAAAA and reverse 5′-GCTCGGAGCTCCCTCTCTAT; SREBP-1c, forward 5′-TGAGAAGCGCTACCGGGCTGCTATCAATGACAAGATTGT-3′ and reverse 5′-CTCCACTGCCACAAGCTGCCACCAGGTCCTTCAGTG-3′; FAS, forward 5′-GCTGCGGAAACTTCAGGAAAT-3′ and reverse 5′-AGAGACGTGTCACTCCTGGACT-3′; ACC1α, forward 5′-GCGGGAGGAGTTCCTAATTC-3′ and reverse 5′-TGTCCCAGACGTAAGCCTTC-3′; mChREBP, forward 5′-CAACCCCTTTCTGAGCTCTGA-3′ and reverse 5′-ctctaagccatgcaccttgaca-3′; mCYP7A1, forward 5′-GAGCCCTGAAGCAATGAAAG-3′ and reverse 5′-GCTGTCCGGATATTCAAGGA-3′.

Confocal Microscopy—Confocal microscopy was performed as described previously (1). Briefly, HeLa cells were grown on uncoated glass coverslips and transfected with pEGFP-DAX-1 and pCDNA3/HA-LXRα by the Lipofectamine method (Invitrogen). 24 h after transfection, cells were fixed with 3.7% formaldehyde for 40 min, mounted on glass slides, and observed with a laser-scanning confocal microscope (Olympus Corp., Lake Success, NY). For detection of pCDNA3/HA-LXRα, cells were permeabilized with 2 ml of PBS containing 0.1% Triton X-100 and 0.1 M glycine at room temperature, incubated for 15 min, washed three times with 1× PBS, and blocked with 3% (w/v) bovine serum albumin in PBS for 10 min at room temperature. Cells were directly incubated with primary anti-HA antibody (1) for 1 h at room temperature, washed three times with 1× PBS, and then mounted on the slide and observed under a microscope.

In Vivo Immunofluorescent Staining—Paraffin sections were used for immunofluorescence staining. After deparaffinizing in xylene and rehydration, the sections were treated with sodium citrate buffer (pH 6.5) and microwaved for 15 min. After cooling for 30 min at room temperature, the sections were incubated with 3% bovine serum albumin for 1 h. The tissue sections were incubated overnight at 4 °C with rabbit polyclonal anti-DAX-1 (1:75; H-300, Santa Cruz Biotechnology, Santa Cruz, CA) and mouse polyclonal anti-LXRα antibody (1:75; H-171, Santa Cruz Biotechnology). Alexa Fluor 488 nm rabbit monoclonal anti-mouse antibody (1:200; Invitrogen) and 546 nm goat monoclonal anti-rabbit antibody (1:200; Invitrogen) were then applied for 1 h at room temperature in the dark. After each step, slides were washed three times for 5 min in PBS. The coverslips were then mounted by ProLong Gold Antifade reagent (Invitrogen) and analyzed under a dual fluorescence microscope (LSM 510 META; Carl Zeiss, Jena, Germany). Control slides were processed the same way, except for omission of the primary antibodies.

Western Blot Analysis—Western blot analysis was performed as described previously (1, 26). Briefly, HepG2 cells were transfected with the indicated expression vectors or small interfering RNA oligonucleotides. Forty eight hours after transfection, cell lysates were prepared and separated on 12% SDS-polyacrylamide gel. At about 80% confluency, H4IIE and rat primary hepatocytes were treated with insulin. The cells were then harvested at different time points, and proteins were transferred to a nitrocellulose membrane (Amersham Biosciences). The membranes were probed with an anti-HA, FLAG, DAX-1, or β-actin antibodies and developed after secondary antibody incubation using the ECL kit (Amersham Biosciences) according to the manufacturer's instruction.

MBP Pulldown Assay—MBP pulldown assay was performed according to the method described previously (27). Briefly, FLAG-hLXRα, HA-hDAX-1, HA-hDAX-1-NT, and -LBD were labeled with [^{35}S]methionine using a TNT *in vitro* translation kit (Promega Corp., Madison, WI); hSRC-1 was labeled with cold methionine, according to the manufacturer's instructions. The indicated MBP and MBP-fused proteins were expressed in *Escherichia coli* strain *BL21*(*DE3*) in ZY media (1% tryptone, 0.5% yeast extract, 100 mM KH_2PO_4, 25 mM $(NH_4)_2SO_4$, 0.5% glycerol, 0.05% glucose, 0.2% α-lactose, 1 mM $MgSO_4$) containing 25 mg/liter kanamycin for 1 h, then cultured for 24 h at 18 °C, purified with amylose beads (New England Biolabs), and then used for the *in vitro* protein-protein assays with the indicated [^{35}S]methionine-labeled proteins, as described previously (28). The beads were washed three times with the binding buffer, analyzed by SDS-polyacrylamide gel, and visualized by a phosphorimager analyzer (BAS-1500, Fuji, Japan).

In Vivo Interaction and Coimmunoprecipitation (CoIP) Assays—HepG2 cells grown in Dulbecco's modified Eagle's medium supplemented with 10% fetal bovine serum were plated in 6-well flat-bottomed microplates at a concentration of 2×10^5 cells per well the day before transfection as described previously (1). Briefly, 1 μg of each plasmid was transfected into 293T cells with a calcium phosphate precipitation method. Forty eight hours after transfection, cells were solubilized, and the cleared lysates were mixed with 15 μl of glutathione-Sepharose beads and rotated for 2 h at 4 °C. The bound proteins were eluted by boiling in SDS sample buffer, subjected to SDS-PAGE, and then transferred to polyvinylidene difluoride membranes (Millipore Corp., Bedford, MA). The membranes were probed with anti-HA or anti-GST antibody and then developed using the ECL kit. For coimmunoprecipitation assays, 750 μg of total protein extract from fasted (12 h) or refed (12 h) mouse livers were immunoprecipitated using DAX-1 (H-300, Santa Cruz Biotechnology) antibody and anti-rabbit IgG beads (Trueblot, eBioscience). Then Dax-1 and Lxrα proteins were detected by Western blot analysis using DAX-1 or LXRα (PPZ0412, Abcam) antibodies and with respective secondary antibodies. Signals were detected with ECL-Plus (Amersham Biosciences).

Chromatin Immunoprecipitation Assay—The chromatin immunoprecipitation assay was performed as described previously (1). Cells were fixed with 1% formaldehyde and further processed using chromatin immunoprecipitation assay kit (Upstate), as described previously (1). Soluble chromatin was immunoprecipitated with anti-DAX-1 (H-300, Santa Cruz Biotechnology), LXRα (Abcam), and SRC-1α (sc8995, Santa Cruz Biotechnology) acetyl-histone H3 (Lys-9) antibodies (catalog number 9671 Cell Signaling Technology). After purification, DNA samples were quantified by quantitative real time PCR using two pairs of primers encompassing the proximal (−267/−8 bp) or distal (−1470/−1210 bp) region of the mouse *SREBP-1C* promoter. The primers used for PCR are as follows: proximal, forward 5′-TGGTTGCCTGTGCGGCAG and reverse 5′-TCAGGCCCCGCCAGGCTTTAA; distal, forward 5′-GCTGGATGTCCAGGCTGAG and reverse 5′-CCAGAGGTATGCAAGCAGA.

Statistical Analyses—Results are shown as means ± S.D. The comparison of different groups was carried out using two-tailed unpaired Student's *t* test, and differences at or under $p < 0.05$ were considered statistically significant and reported as in the figure legends.

RESULTS

DAX-1 Inhibits the Transcriptional Activity of LXRα—We have recently reported that DAX-1 is expressed in liver and represses the transcriptional activity of LXRα to negatively regulate gluconeogenesis (1). To further support the notion that DAX-1 is significantly expressed in liver, we have examined the expression pattern of DAX-1 using both mouse tissue samples and liver cell lines. Our Western blot analysis using mouse tissue samples indicates that DAX-1 is moderately expressed in liver when compared with testis. In addition, we have performed Western blot analysis using two different doses of protein extracts from different cell lines, and this result indicates that DAX-1 is expressed in hepatoma cells such as HepG2, Hepa1c1c7, and H4IIE (Fig. 1*A*). To confirm whether DAX-1 has any effect on other important liver-specific factors, we have performed transient transfection assays using LXRα and its specific reporter or in combination with DAX-1. We found that DAX-1 dose-dependently decreased the reporter activity containing the LXR-binding site (LXRE-Luc) induced by LXRα in the presence of its synthetic agonist T0901317 (Fig. 1*B*). Transfection of DAX-1 also inhibits the basal and LXRα-mediated reporter activity. We have also confirmed the similar effect in 293T cells indicating that this repressive effect is not cell type-specific (Fig. 1*C*). Western blot analysis showed that increase in FLAG-DAX-1 protein did not affect the expression level of HA-LXRα indicating that this repressive effect was not due the reduction in LXRα protein level (Fig. 1*D*). To investigate the effect of endogenous DAX-1 on LXRα transactivity, we knocked down the endogenous *DAX-1* using small interfering RNAs. Knockdown of endogenous *DAX-1* further significantly increased LXRα-mediated transactivity in HepG2 cells (Fig. 1*E*). We have also confirmed that transfection of siDAX-1-2 significantly decreased the endogenous DAX-1 protein level, whereas control siDAX-1-1 did not decrease the expression of DAX-1 (Fig. 1*F*). Overall, these results indicate that DAX-1 is expressed in liver, and it inhibits the transcriptional activity of LXRα.

DAX-1 Interacts and Colocalizes with LXRα—To determine whether the LXRα repression by DAX-1 is mediated through a direct physical interaction, we have performed *in vitro* MBP pulldown assay. MBP alone, MBP-DAX-1, and MBP-SHP were bacterially expressed and incubated with translated *in vitro* ^{35}S-labeled LXRα WT or LXRαΔAF2 proteins. LXRα was found to interact with MBP-DAX-1 but not with MBP alone. Interestingly, the interaction was increased significantly in the presence of LXRα agonist when compared with vehicle alone. As expected, interaction of LXRα with MBP-hSHP was significantly increased in the presence of ligand (supplemental Fig. 1) (28). To further confirm this interaction *in vivo*, we performed *in vivo* GST pulldown assay by transfecting GST (pEBG) or GST-DAX-1 (pEBG-DAX-1) with HA-LXRα. After GST purification, HA-LXRα was detected in the coprecipitates only when coexpressed with GST-DAX-1 but not with the negative control GST alone (Fig. 2*A*). To examine the interaction between endogenous DAX-1 and LXRα, we performed coimmunoprecipitation assay using DAX-1 and LXRα antibodies. Our results indicated that interaction between DAX-1 and LXRα was modestly increased after the treatment of synthetic LXR agonist (Fig. 2*B*). Next, we performed coimmunoprecipitation assay using normal mouse liver to show the endogenous interaction between DAX-1 and LXRα in mouse liver. We immunoprecipitated the liver extract using DAX-1 antibody and performed Western blotting using LXRα antibody. We found that LXRα was coimmunoprecipitated with DAX-1 but not with IgG alone indicating that DAX-1 interacts with LXRα *in vivo* (Fig. 2*C*). To investigate whether DAX-1 and LXRα are colocalized in the same subcellular compartment, we performed confocal microscopic analysis in HeLa cells. Expression vectors for GFP-DAX-1 and HA-LXRα were transfected alone or together in the presence and absence of ligand. As expected, both DAX-1 and LXRα were primarily localized in the nucleus when they were transfected alone (1, 17). In addition, these two proteins were colocalized in the nucleus when they were transfected together both in the absence or presence of agonist (Fig. 2*D*). To further confirm the colocalization of DAX-1 and LXRα in liver, we performed immunofluorescent staining using normal mouse liver sections. We have observed the nuclear colocalization of DAX-1 and LXRα from merged image indicating that these two proteins are colocalized in the nucleus of mouse hepatocytes (Fig. 2*E*). Taken together, these results demonstrate that DAX-1 physically interacts with LXRα *in vivo*, and they are colocalized in the nucleus.

Mapping of Interaction Domain between DAX-1 and LXRα—To map the interaction domain of LXRα with DAX-1, we performed MBP pulldown assay. As shown in Fig. 3*A* (*upper panel*), we generated four deletion constructs of LXRα fused to the N-terminal domain (LXRα AB), DNA binding domain (LXRα C), hinge and ligand binding domain (LXRα DE), and without activation function-2 domain (LXRα DEΔAF-2). *In vitro* translated and ^{35}S-labeled HA-DAX-1 was incubated with bacterially expressed MBP alone or MBP-fused LXRα deletion constructs. We observed that LXRα DE and DEΔAF-2 showed strong interaction with HA-DAX-1 when compared with

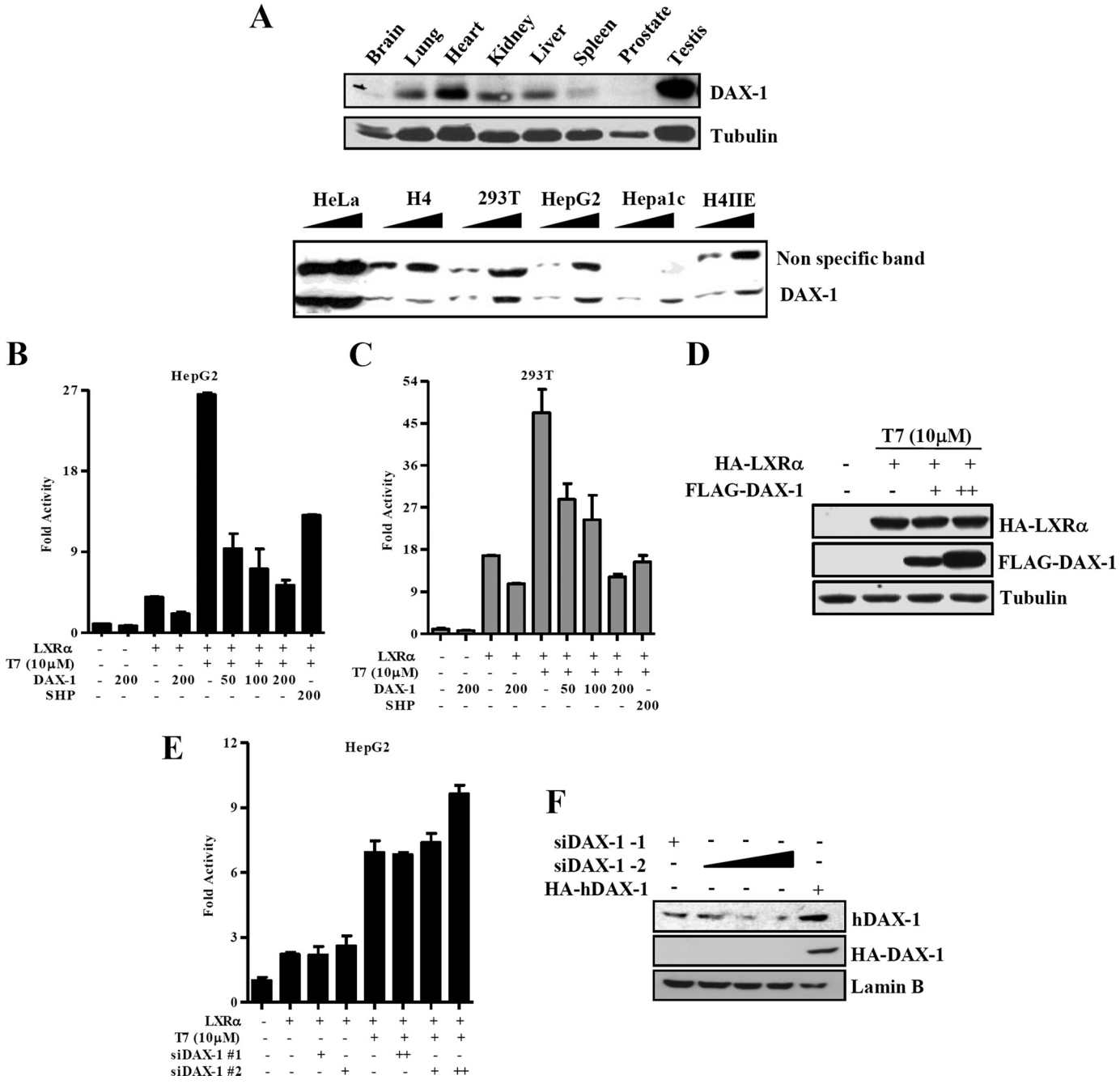

FIGURE 1. **DAX-1 represses the transcriptional activity of LXRα.** *A,* Western blot analysis. Western blot analysis was performed using the protein extracts from mouse tissues (*upper panel*) and cell lines (*lower panel*). *B* and *C,* HepG2 (*B*) and 293T (*C*) cells were transfected with pcDNA3-HA-LXRα (200 ng), HA-DAX-1(50, 100, and 200 ng), and LXRE-luc (200 ng). As positive control, we transfected HA-SHP and HA-LXRα and LXRE-luc in the presence of ligand. Effect of DAX-1 alone with basal reporter activity was also shown. *D,* 293T cells were transfected with HA-LXRα (10 μg) and FLAG-hDAX-1 (5 and 10 μg). *E,* HepG2 cells were transfected with sihDAX-1-1 (200 pmol) or sihDAX-1-2 (50 and 200 pmol), and 24 h later HA-LXRα (200 ng) and LXRE-Luc (200 ng) were transfected. After 24 h, the cells were harvested, and luciferase and β-galactosidase assays were performed. *F,* HepG2 cells were transfected with sihDAX-1-1 (200 pmol) and sihDAX-1-2 (50, 100, and 200 pmol). After 48 h transfection cells (*D* and *E*) were harvested for Western blot analysis with the indicated antibodies.

LXRα WT both in the absence and presence of ligand, whereas weak or no interaction was observed in the cases of LXRα C and AB (Fig. 3*A*, *lower panel*). These results indicate that DAX-1 interacts mainly with LBD and the hinge region of LXRα. In addition, we have also performed similar experiment using *in vitro* translated SRC-1, and the results indicate that the hinge and LBD region of LXRα was involved the interaction with SRC-1 in the presence of ligand. Conversely, when we performed reciprocal mapping experiments using deletion constructs of DAX-1 (Fig. 3*B*, *upper panel*), all ^{35}S-labeled translated DAX-1 proteins interacted with MBP-LXRα (Fig. 3*B*, *lower panel*), indicating that the entire DAX-1 protein is involved in the interaction with LXRα. It has been reported previously that the first L*XX*LL motif of DAX-1 is more essential for the interaction as well as nuclear accumulation of DAX-1 (30) than other two L*XX*LL motifs. Therefore, we made the first L*XX*LL motif mutant DAX-1 (HA-DAX-1 mL1) (Fig. 3*C*, *upper panel*). We performed the interaction assay using

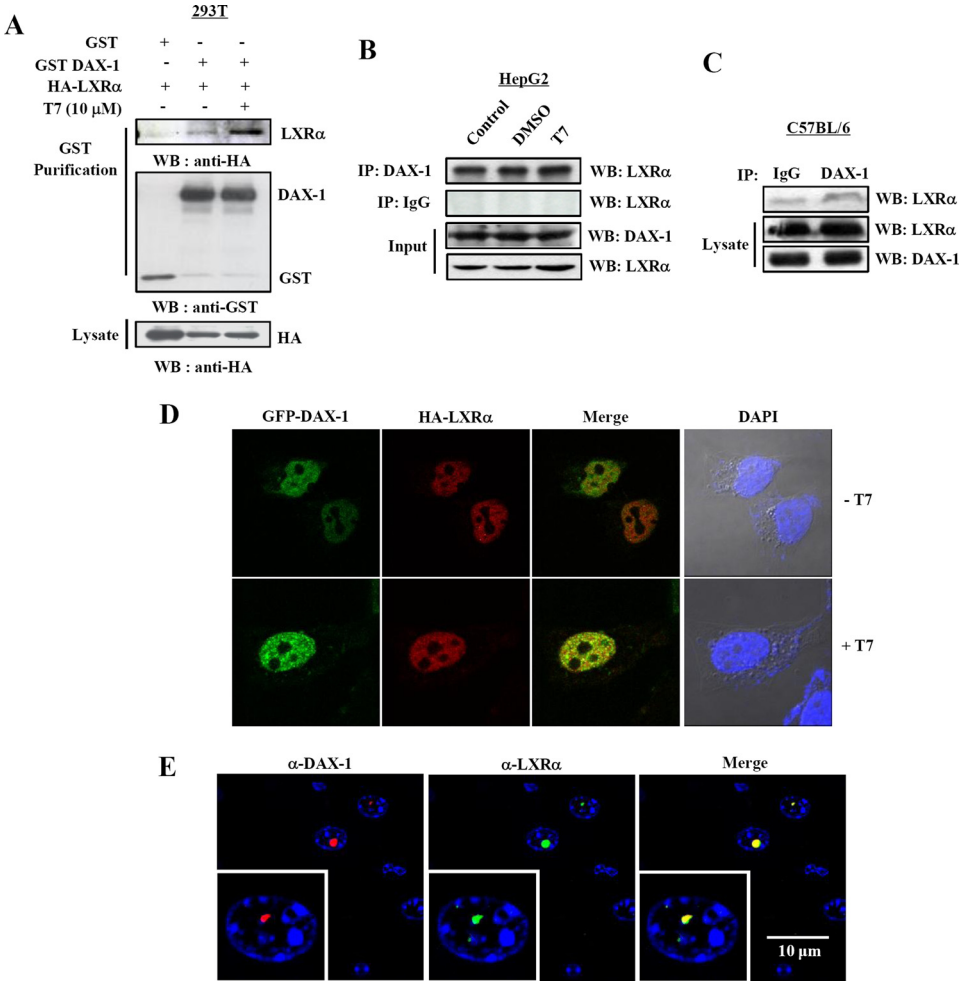

FIGURE 2. **Interaction between DAX-1 and LXRα both *in vitro* and *in vivo*.** *A, in vivo* interaction between DAX-1 and LXRα. 293T cells were cotransfected with expression vectors for HA-LXRα together with pEBG-DAX-1 (GST-DAX-1) or GST alone (pEBG) as a control. The complex formation (*upper panel, GST purification.*) and the amount of HA-LXRα used for the *in vivo* binding assay (*lower panel*, *Lysate*) were determined by anti-HA antibody. The same blot was stripped and re-probed with an anti-GST antibody (*middle panel*) to confirm the expression levels of the GST fusion protein (*GST-hDAX-1*) and the GST control (*GST*). *WB*, Western blot. *B,* endogenous interaction between LXRα and DAX-1 in HepG2 cells. Protein extracts from HepG2 cells treated with vehicle (DMSO) or T7 were coimmunoprecipitated (*IP*) using DAX-1 antibody or secondary antibody alone (negative control) and Western blotted with LXRα antibody. Inputs (10%) for DAX-1 and LXRα are shown in the *bottom panels*. *C,* coimmunoprecipitation assays with liver extracts ($n = 4$) demonstrate the functional association between LXRα and DAX-1. Protein extracts from livers were immunoprecipitated using DAX-1 antibody or IgG alone (negative control) and Western-blotted with LXRα (*upper two panels*) antibody. Expression of LXRα and DAX-1 (*lower two panels*) from 10% of lysate were analyzed by Western blotting with specific antibodies. *D,* subcellular localization of DAX-1 and LXRα. HeLa cells were transiently transfected with pEGFP-DAX-1 or pEGFP with pCDNA3/HA-LXRα. The *yellow* stain in the merged image indicates the colocalization of DAX-1 and LXRα. Data shown are representative cells from one of three independent experiments. *DAPI,* 4′,6-diamidino-2-phenylindole. *E, in vivo* immunofluorescent staining. Paraffin sections of normal (*ad libitum*) mouse liver samples were used for immunofluorescent staining. The hepatic DAX-1 and LXRα proteins were detected with anti-DAX-1 and LXRα antibodies and visualized with *red fluorescence* for DAX-1 and *green fluorescence* for LXRα. Pictures are shown at ×400 magnification with a confocal microscope.

bacterially expressed MBP-LXRα with HA-DAX-1 mL1 (first L*XX*LL motif mutant) and DAX-1 WT. No significant change in interaction was observed between LXRα and DAX-1 mL1 compared with DAX-1 WT (Fig. 3*C*, *lower panel*). Moreover, all these DAX-1 deletion and mutant constructs inhibited the transcription activity of LXRα similar to DAX-1 WT (supplemental Fig. 2) indicating that this interaction is independent of the DAX-1 L*XX*LL motif. Overall, these mapping results indicate that the entire structure of DAX-1 is involved in the interaction with LBD and hinge region of LXRα.

DAX-1 Competes for and Represses Binding of SRC-1 to LXRα—It has been reported that SRC-1 can coactivate the transcriptional activity of LXRα (17). To investigate the functional mechanism of LXRα repression by DAX-1, we performed competition experiments using the LXRα coactivator SRC-1. HepG2 cells were transfected using LXRE-Luc and LXRα expression vector with different combinations of expression vectors for DAX-1 and SRC-1. We have found that the transcriptional activity of LXRα was coactivated by the transfection of SRC-1, and it was decreased significantly by DAX-1 in a dose-dependent manner. However, DAX-1 repression was significantly released by SRC-1 in a dose-dependent manner (Fig. 4*A*). Furthermore, we performed *in vitro* MBP competition assay to confirm competition between DAX-1 and SRC-1 for binding to LXRα *in vitro*. Increasing amounts of unlabeled full-length SRC-1 competed with ^{35}S-labeled DAX-1 for the binding with MBP-LXRα. However, the weak interaction between ^{35}S-labeled DAX-1 and MBP-LXRα CT was not altered by the incubation of unlabeled SRC-1 (Fig. 4*B*). Altogether, these results indicate that DAX-1 competes with SRC-1 for the binding to LXRα to repress LXRα transactivation.

DAX-1 Decreases Agonist-induced LXRα Target Gene Promoter Activity and Expression—Next, we examined whether DAX-1 can inhibit the activity of natural LXRα target gene promoter. HepG2 cells were transfected with the LXRα target gene promoter SREBP-1c-Luc and an expression plasmid for DAX-1 and were treated with the LXRα agonist. DAX-1 inhibited T7-mediated SREBP-1c-Luc activity in a dose-dependent manner, indicating that DAX-1 can also inhibit LXRα-target gene promoter activity (Fig. 5*A*). To examine whether this inhibition was achieved by direct recruitment of DAX-1 on the *SREBP-1c* promoter, we performed endogenous chromatin immunoprecipitation assay in rat primary hepatocytes in the absence or presence of ligand with or without the infection of Ad-DAX-1. We could find a minimal recruitment of DAX-1 on the LXRα binding region of the SREBP-1c promoter in the absence of ligand, whereas this

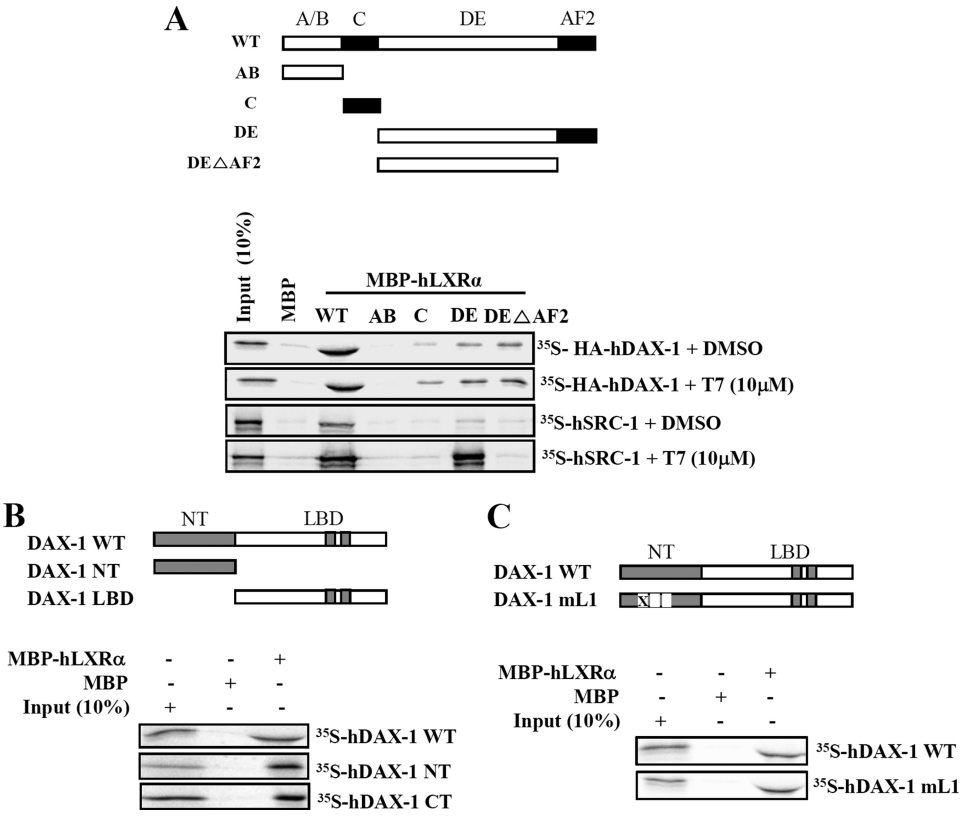

FIGURE 3. **Mapping of interaction domain between DAX-1 and LXRα.** *A,* schematic representation of LXRα deletion constructs (*upper panel*). *In vitro* MBP pulldown assay was performed using bacterially expressed various MBP-LXRα deletion constructs and ^{35}S-labeled HA-DAX-1 WT (*lower panel*). *B,* schematic representation of DAX-1 deletion constructs (*upper panel*). *In vitro* MBP pulldown assay was performed using bacterially expressed MBP-LXRα WT and *in vitro* translated ^{35}S-labeled different HA-DAX-1 deletion constructs. Then cell lysates were immunoprecipitated with amylose beads and detected using phosphorimager (*lower panel*). *NT*, N terminus; *CT*, C terminus. *C,* schematic representation of DAX-1 WT and DAX-1 mL1 (mutant of first LXXLL motif) constructs (*upper panel*). MBP pulldown assay was performed using bacterially expressed MBP-LXRα WT and *in vitro* translated ^{35}S-labeled HA-DAX-1 WT and HA-DAX-1 mL1 proteins. The cell lysates were then immunoprecipitated with amylose beads and detected using phosphorimager (*lower panel*).

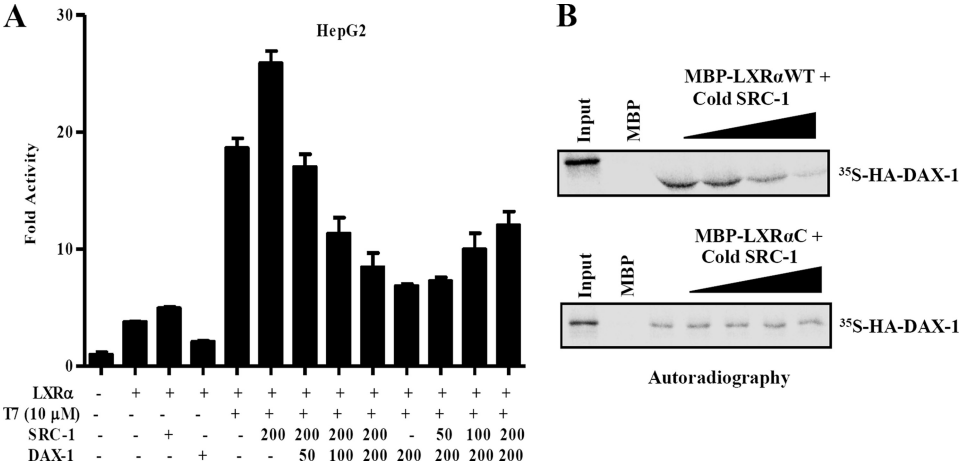

FIGURE 4. **DAX-1 competes with SRC-1 for LXRα transactivation.** *A,* HepG2 cells were transfected using 200 ng of LXRE-Luc with indicated amounts of LXRα, SRC-1, and DAX-1 expression vectors. Cells were harvested 40 h after transfection, and lysates were utilized for luciferase and β-galactosidase assay. The results shown are the mean of β-galactosidase values from three independent experiments. Effects of DAX-1 and SRC-1 alone on the basal reporter activity are also shown. *B, in vitro* MBP competition assay. MBP-fused full-length LXRα (*upper panel*) or MBP-LXRαC (*lower panel*) bound to amylose beads was incubated with ^{35}S-labeled full-length HA-hDAX-1, in the presence of increasing amounts of cold methionine-labeled SRC-1 (1, 2, 4, or 8 μl). After washing, bound proteins were subjected to SDS-PAGE, and the amount of MBP-bound HA-DAX-1 was visualized via autoradiography.

recruitment was totally abolished in the presence of the LXRα agonist. As expected, the recruitment of LXRα, SRC-1, and acetylated lysine 9 of histone H3 was significantly increased after the treatment of LXRα agonist. However, the recruitment of these proteins was significantly decreased by the infection of adenovirus DAX-1. These results suggest the existence of competition mechanism between DAX-1 and SRC-1 for repression of the LXRα transactivation (Fig. 5*B*). To confirm whether DAX-1 can also decrease the expression of LXRα target genes, we infected adenovirus DAX-1 (Ad-DAX-1) in HepG2 and rat primary hepatocytes. We found that infection of Ad-DAX-1 dose-dependently decreased T7-induced expression of LXRα target genes, *SREBP-1c* and FAS (Fig. 5, *C* and *D*). We further examined the effect of DAX-1 on down-regulating the LXRα target gene expression by performing adenovirus-mediated knockdown experiments. Infection of adenovirus-expressing short hairpin RNA for DAX-1 (Ad-sh-DAX-1) significantly abolished the endogenous DAX-1 expression compared with a control virus (Ad-US). Knockdown of endogenous *DAX-1* significantly increased the expression of T7-mediated *SREBP-1c* and FAS gene expression (Fig. 5*E*). Overall, these results indicate that DAX-1 can down-regulate the LXRα target gene expression in both the liver cell line and rat primary hepatocytes.

DAX-1 Decreases Triglyceride Level and Lipid Accumulation in Liver—To assess the functional consequences of the down-regulation of T7-mediated lipogenic genes by DAX-1, we first examined the expression of *DAX-1* and LXRα target genes in normal and obese-diabetic (*db/db*) mice. As reported previously (31), *Srebp-1c*, FAS, and acetyl-coenzyme A carboxylase were significantly higher in *db/db* mice compared with normal mice, whereas the expression of DAX-1 was significantly low in *db/db* mice compared with normal mice (Fig.

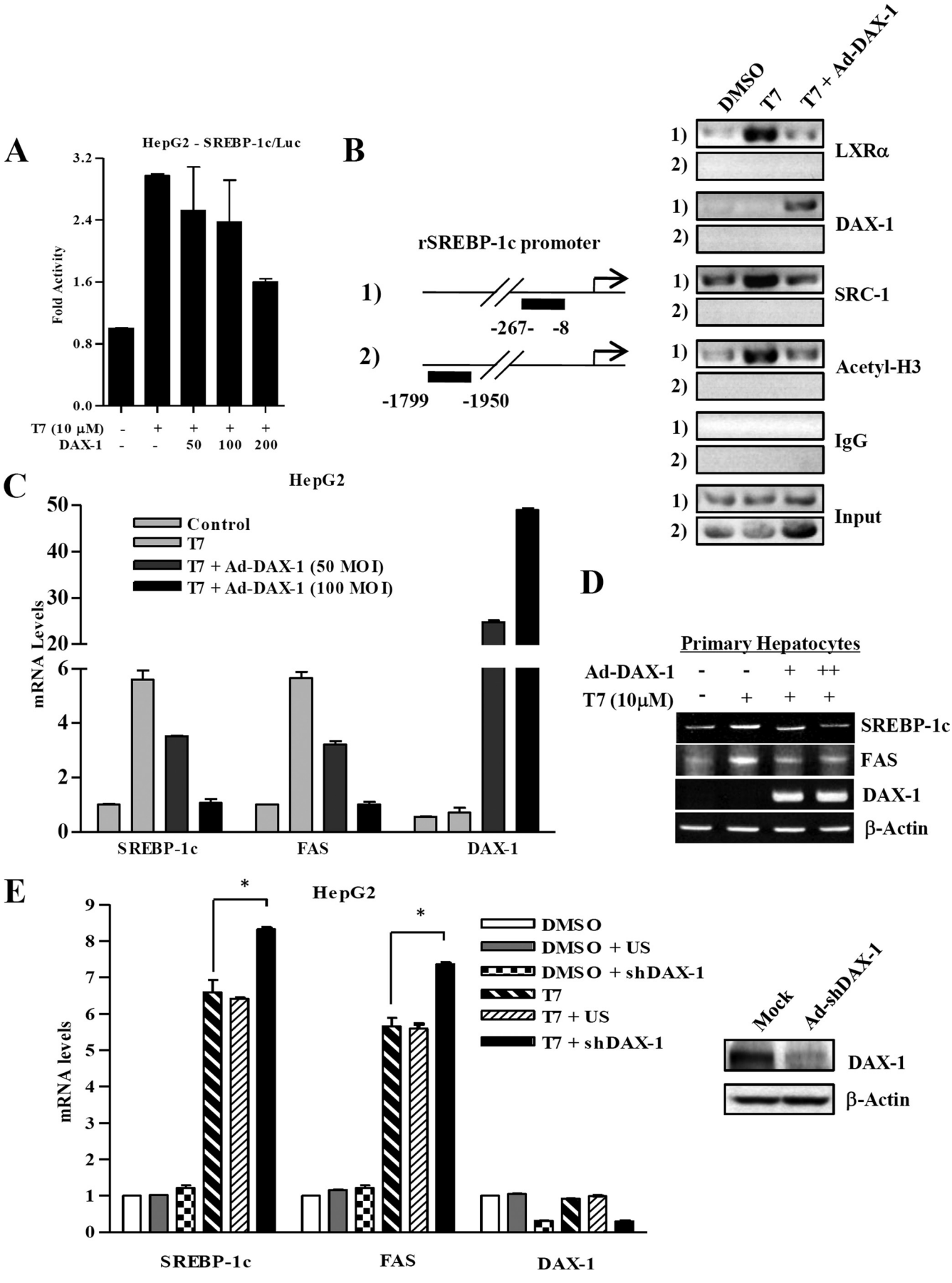
A
HepG2 - SREBP-1c/Luc
Fold Activity
3.2
2.4
1.6
0.8
0.0
T7 (10 μM) - + + + +
DAX-1 - - 50 100 200
B
rSREBP-1c promoter
1)
-267- -8
2)
-1799 -1950
DMSO
T7
T7 + Ad-DAX-1
LXRα
DAX-1
SRC-1
Acetyl-H3
IgG
Input
C
HepG2
Control
T7
T7 + Ad-DAX-1 (50 MOI)
T7 + Ad-DAX-1 (100 MOI)
mRNA Levels
SREBP-1c
FAS
DAX-1
D
Primary Hepatocytes
Ad-DAX-1 - - + ++
T7 (10μM) - + + +
SREBP-1c
FAS
DAX-1
β-Actin
E
HepG2
mRNA levels
DMSO
DMSO + US
DMSO + shDAX-1
T7
T7 + US
T7 + shDAX-1
SREBP-1c
FAS
DAX-1
Mock
Ad-shDAX-1
DAX-1
β-Actin

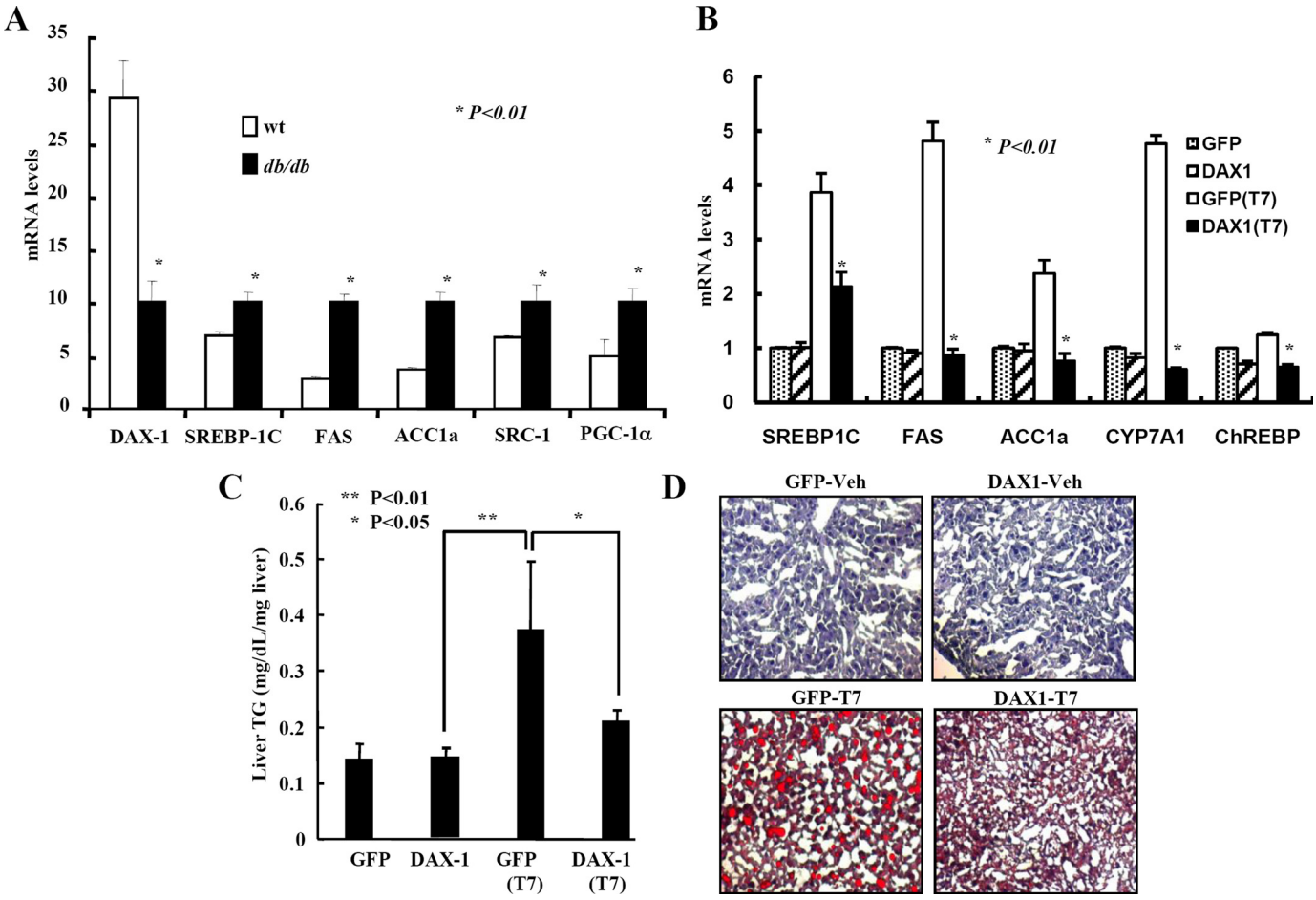

FIGURE 6. **DAX-1 lowers serum triglyceride and lipid accumulation in liver.** Comparison of DAX-1 and lipogenic gene expressions in normal and *db/db* mice. *A,* quantitative PCR analysis of hepatic mRNA levels of DAX-1, SRC-1, PGC-1a, SREBP-1C, FAS and acetyl-coenzyme A carboxylase in normal and *db/db* mice (*, $p < 0.01$; $n = 4$). *B,* DAX-1 decreases T7-mediated lipogenic gene expression in mice. Male 8-week-old C57BL6 mice were provided with the meal form of a standard rodent diet. T0901317 (LXR agonist, 50 mg/kg body weight) or vehicle (1% methylcellulose and 1% Tween 80) were administered by oral gavage each day for 1 week. Recombinant adenovirus (0.5×10^9 plaque-forming unit) GFP ($n = 5$) or DAX-1 ($n = 5$) were delivered by tail vein injection on the 4th day of oral gavage. Three days after adenovirus GFP ($n = 3$) or DAX-1 ($n = 3$) injection, mice were sacrificed, and the expressions of SREBP-1c, FAS, and ACC1α were analyzed by real time quantitative RT-PCR. All data were normalized to ribosomal L32 expression. *C,* liver triglyceride level is decreased by DAX-1. Hepatic TAG levels were analyzed from mouse liver tissue infected with adenoviruses as in *B. D,* DAX-1 decreases the lipid accumulation in liver. Oil Red O staining was performed from the liver samples as in *B*. Data in *A–C* are represented as mean ± S.D.

6*A*). These results indicate that there was an inverse correlation between *DAX-1* and LXRα target gene expression in the livers of normal and *db/db* mice. Next, we treated the normal mice with LXRα agonist for 7 days and performed a tail vein injection of Ad-DAX-1. We found that LXRα target genes were significantly increased after the treatment of the LXR agonist, and it was drastically decreased by the infection of Ad-DAX-1. We also examined other LXRα target genes such as *Cyp7a1* and ChREBP. We observed that agonist-induced both *Cyp7a1* and ChREBP were significantly decreased by the infection of Ad-DAX-1 (Fig. 6*B*). We had also observed that T7-mediated induction of nuclear SREBP-1c and acetyl-coenzyme A carboxylase protein levels were decreased (supplemental Fig. 3) in the liver extracts infected with Ad-DAX-1. Consistent with the decrease in lipogenic gene expression, T7-induced liver triglyceride levels were also decreased after DAX-1 expression (Fig. 6*C*). However, plasma cholesterol and triglyceride levels were not significantly changed by adenovirus tail vein injection (supplemental Fig. 4). Finally, we tried to find out whether DAX-1 can decrease the lipid accumulation in liver. We per-

FIGURE 5. **DAX-1 decreases LXRα agonist-mediated target gene promoter activity and expression.** *A,* HepG2 cells were transfected with SREBP-1c-Luc and with LXRα and DAX-1, and cell lysates were utilized for luciferase and β-galactosidase assays. The results shown are means of β-galactosidase values from three independent experiments. *B,* chromatin immunoprecipitation analysis using antibodies for LXRα, DAX-1, SRC-1, and acetyl-H3. PCR amplification of immunoprecipitated chromatin fragments was conducted using primer pairs specific for the proximal, regulatory region (*1*) and a distal, nonregulatory region (*2*) of the SREBP-1C gene promoter (*left panel*). Cell extracts from primary hepatocytes treated with vehicle (DMSO) or LXRα agonist (T7) with or without infection of Ad-DAX-1 were immunoprecipitated with LXRα, DAX-1, SRC-1, and acetyl-H3 antibodies (*right panel*). After reverse cross-linking, DNA was extracted, and PCR was performed using primers for LXR-RE containing proximal and nonspecific distal region of SREBP-1c promoter. As a negative control, cell extracts were incubated with IgG without any preincubation of primary antibody. Inputs (5%) for both proximal and distal SREBP promoter are shown. *C* and *D,* quantitative PCR analysis was performed using total RNA extracted from HepG2 (*C*), and RT-PCR analysis was performed using total RNA from rat primary hepatocytes (*D*) after the treatment of LXRα agonist with or without adenovirus DAX-1 infection. DAX-1, SREBP-1C, FAS, and β-actin genes amplified using specific primers for DAX-1, SREBP-1C, FAS, and β-actin were used for PCR. *E*, Student's *t* test. Western blot analysis showing protein level of DAX-1 from HepG2 cells infected with mock and Ad-shDAX-1 (*right panel*).

formed Oil Red O staining using a mouse liver sample treated with vehicle alone or T7-treated mice with either Ad-GFP or Ad-DAX-1 infection. A significant decrease in T7-mediated lipid accumulation was observed in livers of mice with Ad-DAX-1 infection (Fig. 6*D*) indicating that DAX-1 can decrease T7-mediated lipid accumulation in liver. Overall, these results suggest that DAX-1 can control the LXR agonist-mediated lipogenesis in liver.

DISCUSSION

We have recently demonstrated that DAX-1 is expressed in liver and controls the gluconeogenesis by inhibiting the transcriptional activity of HNF4α (1). In this study, our expression analysis in different tissues and cell lines has further supported our previous evidence that DAX-1 is significantly expressed in liver. We have also found that DAX-1 can inhibit the transcriptional activity of another liver-enriched nuclear receptor LXRα. This has been achieved by direct physical interaction as well as the competition with LXRα coactivator SRC-1. Overexpression of DAX-l significantly decreases the LXR agonist-mediated induction of target gene expression, whereas knockdown of endogenous DAX-1 significantly increases the expression of LXRα target genes such as *SREBP-1c* and FAS. Finally, we observed that adenovirus-mediated expression of DAX-1 significantly decreased T7-mediated induction of lipogenic genes and lipid accumulation in liver. Altogether, this study suggests that DAX-1 can control the lipogenesis by inhibiting the transcriptional activity of LXRα in liver.

Although DAX-1 has been shown to be primarily expressed in gonads and adrenal glands, there are some reports showing the existence of DAX-1 in the liver (32–34). Our expression analyses in different tissues samples of mice and in cell lines have also provided more evidence that DAX-1 is expressed in liver. Our previous report has also demonstrated that DAX-1 can control hepatic gluconeogenesis by inhibiting the transcriptional activity of HNFα (1). Consistent with our previous report, we have found that DAX-1 can also inhibit the transcriptional activity of another liver-specific receptor LXRα. Similar to this DAX-1-mediated repressive effect, the closely related family member SHP has also been to shown to inhibit the transcriptional activity of LXRα (28). We have found the repressive effect of DAX-1 was not cell type-specific, reminiscent of our previous reports that the DAX-1-mediated transcriptional repression of HNF4α and PPARγ was not cell type-specific (1, 12).

Next, we have shown the physical interaction between DAX-1 and LXRα both *in vitro* and *in vivo*. This direct interaction was increased in the presence of the LXR agonist, which is also consistent with the previous study that the interaction between SHP and LXRα was stronger in the presence of LXR agonist (28). This increase in interaction might be due to the increased expression and stability of the LXRα protein in the presence of agonist (35, 36). Consistent with these reports, we have also observed an increase in LXRα protein level in the input panel after the treatment of synthetic agonist. Moreover, coactivators and corepressors were known to recognize overlapping surfaces of liganded and unliganded nuclear receptors, respectively. At a sufficiently high concentration, the NCoR has been previously shown to influence the activity of the LXR even in the presence of a potent full agonist that destabilizes NCoR binding (19). In accordance with previous reports (1, 17), DAX-1 and LXRα were predominantly localized in the nucleus when they were expressed alone both in the absence or presence of agonist. These two proteins were colocalized in the nucleus when they were coexpressed both in the absence or presence of agonist. This result strengthens the previous evidence that RIP140 and LXRα were colocalized in the nucleus (37). Our domain mapping results depicted that LBD and the hinge region of LXRα is involved in the interaction with DAX-1 and is consistent with previous reports that SHP and RIP140 interacted with the LBD region of LXRα (28, 38) or DAX-1 interacted with DNA binding domain and hinge region of PPARγ (12). On the other side, the entire DAX-1 protein is involved in the interaction with LXRα, which is also consistent with our previous observation that all the domains of DAX-1 interacted with PPARγ and HNF4α (1, 12). However, the LBD region of DAX-1 was involved in the interaction with Nur77 (11). However, SHP utilized its C-terminal domain for the interaction with LXRα (28). It has been previously reported that DAX-1 has three L*XX*LL motifs in its N-terminal repetitive region and the first L*XX*LL motif was more essential for the interaction as well as nuclear accumulation of DAX-1 than other two motifs (30). In this study, the first L*XX*LL motif mutant did not show any significant change in interaction with LXRα (Fig. 3*C*), and it could still inhibit the LXRα transactivation like wild type DAX-1 (supplemental Fig. 2). We have found that DAX-1 was competing with LXRα coactivator SRC-1 for binding to LXRα in the presence of agonist. Similarly, competition between DAX-1 was shown to be competed with SRC-1 for repressing Nur77 (11). However, DAX-1 competed with coactivators such as PGC-1α and GRIP-1 for repressing the transcriptional activity of PPARγ and glucocorticoid receptor, respectively (10, 12). It has previously been reported that DAX-1 can recruit NCoR to suppress the transcriptional activity of SF-1 (9), and NCoR was also known to repress the transcriptional activity of LXRα (19). Therefore, in addition to the coactivator competition mechanism, DAX-1 may also recruit NCoR to repress LXRα transactivation.

LXRs can directly promote SREBP-1c gene transcription through two LXRE-binding sites in the SREBP-1c promoter (37), and synthetic LXR agonist can up-regulate SREBP-1c gene expression (22). We have found that LXR agonist-mediated *SREBP-1c* promoter activity was decreased by the transfection of *DAX-1*. Similarly, it has been previously reported that agonist-induced LXR target gene promoter *ABCA1* and *SREBP-1c* were significantly repressed by NCoR and SMRT (19). It is well known that the expression of FAS and acetyl-coenzyme A carboxylase can be up-regulated by LXRα synthetic agonist (22). In addition, we have found that LXRα, DAX-1, and SRC-1 were recruited on the LXR binding region of the *SREBP-1c* promoter in the absence of ligand. It is consistent with a previous report that LXR agonist T0901317 significantly increased the binding of LXRα on the *SREBP-1c* promoter (28). In contrast to the recruitment of LXRα, DAX-1, which was recruited to the *SREBP-1c* promoter, was significantly dissociated from the promoter after treatment of the LXRα agonist. This phenomenon is similar to the previous observation that the recruitment of

NCoR was significantly decreased after the treatment of the LXRα agonist (22). In addition, protein kinase A phosphorylation of LXRα has been shown to impair the DNA binding activity by preventing LXRα/RXR dimerization and decreases its transcription activity by inhibiting the recruitment of coactivator SRC-1 and enhancing recruitment of corepressor NCoR (22, 39). We observed the decrease in recruitment of acetylated histone 3 on chromatin structure by the overexpression of DAX-1 indicating that DAX-1 could affect the chromatin structure like SHP (40). Although interaction between DAX-1 and LXRα was increased in the presence of ligand, their recruitments on target gene promoter were inversely correlated.

We have found a significant decrease in LXRα agonist-mediated lipogenic gene expression, triglyceride levels, and lipid accumulation in the liver by DAX-1 expression. Similarly, some reports demonstrated that activation of protein kinase A and protein kinase C decreased LXRα target gene expressions (39, 41), and our previous report suggested that SIK1 can regulate hepatic lipogenesis by controlling SREBP-1c phosphorylation (26). However, the histone deacetylase Sirt1 has been shown to positively regulate LXRα target gene expression (18). Our previous report has suggested that salt inducible kinase 1 (SIK1) can induce DAX-1 gene expression in liver (1). Thus, we are currently investigating whether SIK1-mediated induction of DAX-1 in liver can control the expression of lipogenic genes, including *Srebp-1c*, FAS, and acetyl-coenzyme A carboxylase. LXR is known to regulate the expression of ChREBP, which is also known to directly promote the lipogenic gene transcription (23, 42). Therefore, we are currently exploring whether DAX-1 has any direct effect on ChREBP transactivation. Recently, the crystal structure of DAX-1 has also been elucidated (14), and it has been demonstrated that DAX-1 and SHP can form homodimers as well as heterodimers (43). Similar to DAX-1 regulatory effect, SHP was also shown to decrease the lipogenic gene expression and triglycerides in liver (44). In addition, DAX-1 and SHP had similar regulatory effects to control the cAMP-mediated induction of gluconeogenic genes such as phosphoenolpyruvate carboxykinase and Glc-6-Pase. Overall, DAX-1 behaves like SHP in the liver to negatively regulate gluconeogenesis and lipogenesis by repressing HNF4α and LXRα, respectively (1, 29). Therefore, target-specific combinatorial expression or double knock-out of these two receptors in liver will be useful to understand the molecular mechanisms to control both glucose and lipid metabolism. A search for a potent inducer of DAX-1 will also be necessary to understand the physiological importance of DAX-1 in liver.

In summary, DAX-1 represses the transcriptional activity of LXRα by competing with its coactivator SRC-1, and it has been achieved through the direct physical interaction with LXRα. In addition, DAX-1 decreases LXR agonist-induced expression of lipogenic genes. Overall, this study suggests that DAX-1 acts as a novel corepressor of LXRα and plays a key role in controlling the lipid metabolism in liver.

Acknowledgments—We thank Yong Deuk Kim and YuanBin Xie for technical assistance and helpful discussions. We sincerely thank Prof. Seok-Yong Choi for critical comments and reading of our manuscript.

REFERENCES

1. Nedumaran, B., Hong, S., Xie, Y. B., Kim, Y. H., Seo, W. Y., Lee, M. W., Lee, C. H., Koo, S. H., and Choi, H. S. (2009) *J. Biol. Chem.* **284,** 27511–27523
2. Giguère, V. (1999) *Endocr. Rev.* **20,** 689–725
3. Aranda, A., and Pascual, A. (2001) *Physiol. Rev.* **81,** 1269–1304
4. Iyer, A. K., and McCabe, E. R. (2004) *Mol. Genet. Metab.* **83,** 60–73
5. Zhang, H., Thomsen, J. S., Johansson, L., Gustafsson, J. A., and Treuter, E. (2000) *J. Biol. Chem.* **275,** 39855–39859
6. Moore, J. M., Galicia, S. J., McReynolds, A. C., Nguyen, N. H., Scanlan, T. S., and Guy, R. K. (2004) *J. Biol. Chem.* **279,** 27584–27590
7. Crawford, P. A., Dorn, C., Sadovsky, Y., and Milbrandt, J. (1998) *Mol. Cell. Biol.* **18,** 2949–2956
8. Holter, E., Kotaja, N., Mäkelä, S., Strauss, L., Kietz, S., Jänne, O. A., Gustafsson, J. A., Palvimo, J. J., and Treuter, E. (2002) *Mol. Endocrinol.* **16,** 515–528
9. Park, Y. Y., Ahn, S. W., Kim, H. J., Kim, J. M., Lee, I. K., Kang, H., and Choi, H. S. (2005) *Nucleic Acids Res.* **33,** 6756–6768
10. Zhou, J., Oakley, R. H., and Cidlowski, J. A. (2008) *Mol. Endocrinol.* **22,** 1521–1534
11. Song, K. H., Park, Y. Y., Park, K. C., Hong, C. Y., Park, J. H., Shong, M., Lee, K., and Choi, H. S. (2004) *Mol. Endocrinol.* **18,** 1929–1940
12. Kim, G. S., Lee, G. Y., Nedumaran, B., Park, Y. Y., Kim, K. T., Park, S. C., Lee, Y. C., Kim, J. B., and Choi, H. S. (2008) *Biochem. Biophys. Res. Commun.* **370,** 264–268
13. Sun, C., Nakatake, Y., Akagi, T., Ura, H., Matsuda, T., Nishiyama, A., Koide, H., Ko, M. S., Niwa, H., and Yokota, T. (2009) *Mol. Cell. Biol.* **29,** 4574–4583
14. Sablin, E. P., Woods, A., Krylova, I. N., Hwang, P., Ingraham, H. A., and Fletterick, R. J. (2008) *Proc. Natl. Acad. Sci. U.S.A.* **105,** 18390–18395
15. Repa, J. J., and Mangelsdorf, D. J. (2002) *Nat. Med.* **8,** 1243–1248
16. Collins, J. L., Fivush, A. M., Watson, M. A., Galardi, C. M., Lewis, M. C., Moore, L. B., Parks, D. J., Wilson, J. G., Tippin, T. K., Binz, J. G., Plunket, K. D., Morgan, D. G., Beaudet, E. J., Whitney, K. D., Kliewer, S. A., and Willson, T. M. (2002) *J. Med. Chem.* **45,** 1963–1966
17. Huuskonen, J., Fielding, P. E., and Fielding, C. J. (2004) *Arterioscler. Thromb. Vasc. Biol.* **24,** 703–708
18. Li, X., Zhang, S., Blander, G., Tse, J. G., Krieger, M., and Guarente, L. (2007) *Mol. Cell* **28,** 91–106
19. Hu, X., Li, S., Wu, J., Xia, C., and Lala, D. S. (2003) *Mol. Endocrinol.* **17,** 1019–1026
20. Yu, C., Markan, K., Temple, K. A., Deplewski, D., Brady, M. J., and Cohen, R. N. (2005) *J. Biol. Chem.* **280,** 13600–13605
21. Astapova, I., Lee, L. J., Morales, C., Tauber, S., Bilban, M., and Hollenberg, A. N. (2008) *Proc. Natl. Acad. Sci. U.S.A.* **105,** 19544–19549
22. Grefhorst, A., Elzinga, B. M., Voshol, P. J., Plösch, T., Kok, T., Bloks, V. W., van der Sluijs, F. H., Havekes, L. M., Romijn, J. A., Verkade, H. J., and Kuipers, F. (2002) *J. Biol. Chem.* **277,** 34182–34190
23. Cha, J. Y., and Repa, J. J. (2007) *J. Biol. Chem.* **282,** 743–751
24. Kim, S. W., Park, K., Kwak, E., Choi, E., Lee, S., Ham, J., Kang, H., Kim, J. M., Hwang, S. Y., Kong, Y. Y., Lee, K., and Lee, J. W. (2003) *Mol. Cell. Biol.* **23,** 3583–3592
25. Park, K. G., Min, A. K., Koh, E. H., Kim, H. S., Kim, M. O., Park, H. S., Kim, Y. D., Yoon, T. S., Jang, B. K., Hwang, J. S., Kim, J. B., Choi, H. S., Park, J. Y., Lee, I. K., and Lee, K. U. (2008) *Hepatology* **48,** 1477–1486
26. Yoon, Y. S., Seo, W. Y., Lee, M. W., Kim, S. T., and Koo, S. H. (2009) *J. Biol. Chem.* **284,** 10446–10452
27. Hozoji, M., Munehira, Y., Ikeda, Y., Makishima, M., Matsuo, M., Kioka, N., and Ueda, K. (2008) *J. Biol. Chem.* **283,** 30057–30063
28. Brendel, C., Schoonjans, K., Botrugno, O. A., Treuter, E., and Auwerx, J. (2002) *Mol. Endocrinol.* **16,** 2065–2076
29. Kim, Y. D., Park, K. G., Lee, Y. S., Park, Y. Y., Kim, D. K., Nedumaran, B., Jang, W. G., Cho, W. J., Ha, J., Lee, I. K., Lee, C. H., and Choi, H. S. (2008) *Diabetes* **57,** 306–314
30. Kawajiri, K., Ikuta, T., Suzuki, T., Kusaka, M., Muramatsu, M., Fujieda, K., Tachibana, M., and Morohashi, K. (2003) *Mol. Endocrinol.* **17,** 994–1004
31. Chisholm, J. W., Hong, J., Mills, S. A., and Lawn, R. M. (2003) *J. Lipid Res.*

44, 2039–2048
32. Wang, D. S., Kobayashi, T., Senthilkumaran, B., Sakai, F., Sudhakumari, C. C., Suzuki, T., Yoshikuni, M., Matsuda, M., Morohashi, K., and Nagahama, Y. (2002) *Biochem. Biophys. Res. Commun.* **297,** 632–640
33. Smith, C. A., Clifford, V., Western, P. S., Wilcox, S. A., Bell, K. S., and Sinclair, A. H. (2000) *J. Mol. Endocrinol.* **24,** 23–32
34. Sugita, J., Takase, M., and Nakamura, M. (2001) *Gene* **280,** 67–74
35. Li, Y., Bolten, C., Bhat, B. G., Woodring-Dietz, J., Li, S., Prayaga, S. K., Xia, C., and Lala, D. S. (2002) *Mol. Endocrinol.* **16,** 506–514
36. Kim, K. H., Yoon, J. M., Choi, A. H., Kim, W. S., Lee, G. Y., and Kim, J. B. (2009) *Mol. Endocrinol.* **23,** 466–474
37. Jakobsson, T., Osman, W., Gustafsson, J. A., Zilliacus, J., and Wärnmark, A. (2007) *Biochem. J.* **405,** 31–39
38. Dif, N., Euthine, V., Gonnet, E., Laville, M., Vidal, H., and Lefai, E. (2006) *Biochem. J.* **400,** 179–188
39. Yamamoto, T., Shimano, H., Inoue, N., Nakagawa, Y., Matsuzaka, T., Takahashi, A., Yahagi, N., Sone, H., Suzuki, H., Toyoshima, H., and Yamada, N. (2007) *J. Biol. Chem.* **282,** 11687–11695
40. Gobinet, J., Carascossa, S., Cavaillès, V., Vignon, F., Nicolas, J. C., and Jalaguier, S. (2005) *Biochemistry* **44,** 6312–6320
41. Delvecchio, C. J., and Capone, J. P. (2008) *J. Endocrinol.* **197,** 121–130
42. Ishii, S., Iizuka, K., Miller, B. C., and Uyeda, K. (2004) *Proc. Natl. Acad. Sci. U.S.A.* **101,** 15597–15602
43. Iyer, A. K., Zhang, Y. H., and McCabe, E. R. (2006) *Mol. Endocrinol.* **20,** 2326–2342
44. Watanabe, M., Houten, S. M., Wang, L., Moschetta, A., Mangelsdorf, D. J., Heyman, R. A., Moore, D. D., and Auwerx, J. (2004) *J. Clin. Invest.* **113,** 1408–1418